Part Two
Capillary Electromigration Techniques

7
Capillary Electromigration Techniques: Capillary Electrophoresis

Václav Kašička

7.1
Introduction

Capillary electrophoresis (CE), also called capillary zone electrophoresis (CZE), is the basic and most frequently used technique from the family of capillary electromigration separation methods. A common feature of these methods is that they utilize the differential movement of soluble charged species in the electric field for their separation and that this separation takes place in a liquid medium in thin narrow-bore capillaries usually with a 10–100 μm inner diameter (id), a 150–375 μm outer diameter (od), and 20–100 cm length. The separation principle is rather old; the electrophoretic and electroosmotic phenomena were first reported in 1809 [1] and the basic theory of electrophoresis was established by Kohlrausch in 1897 [2,3]. Nevertheless, the application of electrophoresis as an analytical technique dates back to 1937, when Tiselius developed the so-called "moving boundary electrophoresis". He applied it to the separation of blood serum proteins and was able to distinguish basic fractions of these proteins – albumins, and α-, β-, and γ-globulins [4]. For these achievements, he was awarded the Nobel Prize in 1948. In the 1950s and 1960s of the last century, electrophoresis in a slab gel format was developed and was and is still widely used in biochemistry for analytical and micropreparative separations of proteins, polypeptides, polynucleotides, and nucleic acids [1]. Pioneering electrophoretic separations in a narrow-bore tube format were performed by Hjertén in the 1960s (free zone electrophoresis in a 1–3 mm id glass rotating tube) [5], by Virtanen in the 1970s (free zone electrophoresis in 200-μm id glass capillaries) [6], and by Everaerts *et al.* in the 1970s (isotachophoresis (displacement electrophoresis) and zone electrophoresis in polytetrafluoroethylene 200–450-μm id capillaries) [7,8]. However, the modern era of CE started only in 1981 when Jorgenson and Lukacs performed electrophoretic experiments for the first time in 80–100 cm long open tubular 75/550 μm id/od glass capillaries at a high separation voltage of 30 kV. Using highly sensitive on-column fluorescence detection, an extremely sharp and fast separation of complex mixtures of derivatized peptides, amino acids, and amines, with separation efficiencies above 400 000 theoretical plates, was achieved [9,10].

Analytical Separation Science, First Edition. Edited by Jared L. Anderson, Alain Berthod, Verónica Pino Estévez, and Apryll M. Stalcup.

Since then, CE has been subjected to intensive research and development and nowadays it is accepted as highly sensitive, highly efficient, high-speed, highly selective, and widely applicable method – a recognized complement and/or counterpart of the most spread separation techniques, variable modes of high-performance, ultrahigh-performance, and nanoliquid chromatography (HPLC, UHPLC, and nano-LC, respectively). The aim of this chapter is to provide a brief introduction to the CE method, particularly to introduce the basic concepts and theory of electrophoresis in general, to describe the separation principle and basic experimental setup of CE, to demonstrate the advantages and limitations of CE compared to other methods, to show the dispersion effects in CE and the ways of their minimization, and to emphasize a wide applicability of CE as a highly sensitive analytical method. The limited range of this chapter allows only a brief description of the main issues of CE; for a more detailed study of CE and other capillary electromigration methods (isotachophoresis (CITP), isoelectric focusing (CIEF), affinity electrophoresis (ACE), electrokinetic chromatography (CEKC), and electrochromatography (CEC), altogether sometimes called high-performance capillary electrophoresis – HPCE), several monographs and review articles are recommended [11–20].

7.2 Electrophoresis: Basic Concepts

Electrophoresis is an electrokinetic phenomenon. It is defined as the movement of charged molecular species (ions) or particles in a liquid medium under the influence of an electric field. Based on the different migration velocities of ions and particles differing in their electric charge, size, and shape, electrophoresis has become an important electromigration separation method widely used mainly for analytical but sometimes also for (micro)preparative purposes.

The central magnitude in electromigration methods is electrophoretic mobility. Electrophoretic mobility, m, of an ion or a charged particle is defined as its migration velocity, v_{mig}, related to the electric field of unit intensity:

$$m = v_{mig}/E \quad [m^2/(V\,s)] \tag{7.1}$$

where E (V/m) is the intensity (strength) of the electric field, that is, the applied separation voltage U_{sep} (V) per unit length of the separation compartment (total capillary length in the case of CE) L_{tot} (m):

$$E = U_{sep}/L_{tot} \quad [V/m] \tag{7.2}$$

In the presence of an electric field, the particle possessing an electric charge q (C) experiences (i) the force of the electric field, F_e:

$$F_e = q\,E \quad [N] \tag{7.3}$$

and (ii) the frictional force F_f, which for a spherical particle of radius r (m) is governed by the Stokes law:

$$F_f = -6\,\pi\,\eta\,r\,v_{mig} \quad [N], \tag{7.4}$$

where η (Pa s) is the viscosity of the liquid medium surrounding the particle.

After the application of an electric field, practically immediately a balance between the electric field force and the frictional force is established: $F_e = -F_f$, that is,

$$q\,E = 6\,\pi\,\eta\,r\,v_{mig}. \tag{7.5}$$

The combination of Equations 1.1 and 1.5 gives the relation for electrophoretic mobility:

$$m = v_{mig}/E = q/6\,\pi\eta r. \tag{7.6}$$

This equation shows that the mobility of an ion is directly proportional to its charge and indirectly proportional to its radius (size or relative molecular mass) and the viscosity of the medium.

Mobilities of small ions at their full charged state, at a reference temperature of 25 °C, and extrapolated to infinite dilution (zero ionic strength), are called absolute or limiting ionic mobilities and they represent qualitative physicochemical parameters of the ions. The ionic mobilities at a particular ionic strength and temperature are called actual ionic mobilities. Their dependence on the ionic strength of the solution is rather complex and is described by the extended Debye, Hückel, and Onsager (DHO) theory [21] or by the more advanced Onsager–Fuoss theory [22]. Here, the equation for concentration (ionic strength) dependence of the mobility will be given only for the simple case of an ion of a uni-univalent electrolyte:

$$m = m_0 - \left[\frac{8.204\times10^5}{(\varepsilon_r T)^{3/2}}m_0 + \frac{4.275}{\eta(\varepsilon_r T)^{1/2}}\right]\times\frac{\sqrt{I}}{1+50.29a(\varepsilon_r T)^{-1/2}\sqrt{I}}, \tag{7.7}$$

where m is the actual ionic mobility at the ionic strength I, m_0 is the limiting ionic mobility (mobility at zero ionic strength) ($10^{-9}\,m^2/(V\,s)$), ε_r is the solvent relative permittivity, η is the solvent viscosity (Pa s), and T is the absolute temperature (K) of the surrounding solution, a (in Å, 1 Å = 0.1 nm) is the ionic size parameter, that is, the distance between the ion and the counterion centers, and I is the ionic strength of the solution, defined as

$$I = \frac{1}{2}\sum_i c_i z_i^2, \tag{7.8}$$

where c_i (mol/l) is the concentration and z_i is the charge number of the ith ionic species in the surrounding solution. In CE, this solution is called the background

electrolyte (BGE). Usually, it is a buffered conductive liquid medium (solution of the electrolyte(s)), in which the CE separation occurs.

For showing the temperature dependence of mobility, the following equation is used [23]:

$$m_t = m_{25}[1 + k(t - 25)], \tag{7.9}$$

where m_t is the mobility at temperature t (°C), m_{25} is the mobility at 25 °C, and k is the coefficient of temperature dependence of the viscosity of the solvent; for water between 20 and 35 °C, $k = 0.020$.

For strong electrolytes, the actual ionic mobility is equal to their electrophoretic mobilities as obtained from CE measurements (see Equation 1.21 in Section 1.3.3). For weak electrolytes, the term effective mobility was introduced, which reflects the degree of their dissociation for the particular ionic species. Thus, for example, the effective mobility of the univalent weak acid HA is equal to the product of the ionic mobility of its fully charged anionic form A^-, m_{A-}, and the degree of dissociation (molar fraction of anionic form) of this weak acid, α_{HA}:

$$m_{eff,HA} = m_{A-}\alpha_{HA}, \tag{7.10}$$

where α_{HA} is defined as

$$\alpha_{HA} = c_{A-}/(c_{A-} + c_{HA}). \tag{7.10a}$$

Similarly, the effective mobility of the univalent weak base B is equal to the product of the ionic mobility of its fully protonated form (conjugated acid) BH^+, m_{BH+}, and the degree of dissociation of this conjugated acid, α_{BH+}:

$$m_{eff,B} = m_{BH+}\alpha_{BH+}, \tag{7.11}$$

$$\text{where} \quad \alpha_{BH+} \text{ is} \quad \alpha_{BH+} = c_{BH+}/(c_{BH+} + c_B). \tag{7.11a}$$

The effective mobility of a general weak electrolyte including an ampholyte, m_{eff}, is equal to the sum of products of ionic mobilities, m_i, and molar fractions of the particular ionic species in the given electrolyte, x_i:

$$m_{eff} = \sum_{i=N}^{i=M} m_i x_i, \tag{7.12}$$

where $M \geq 0$ is the maximum positive charge (charge number), $N \leq 0$ is the maximum negative charge (charge number including sign), and the molar fraction x_i is defined as:

$$x_i = c_i / \sum_{i=N}^{i=M} c_i, \tag{7.13}$$

where c_i (mol/l) is the molar concentration of the ith species including noncharged species.

Molar fractions and hence also the effective electrophoretic mobilities and velocities of weak electrolytes and ampholytes are strongly dependent on the pH

of the BGE and on the acidity (ionization) constants of their ionogenic groups. For the effective mobility $m_{\mathrm{eff,A}}$ of the ampholyte A, for example, an amino acid possessing one acidic and one basic group, the following equation can be derived [24]:

$$m_{\mathrm{eff,A}} = \frac{m_{\mathrm{A^+}} 10^{\mathrm{p}K_{\mathrm{a,1}} - \mathrm{pH}} + m_{\mathrm{A^-}} 10^{\mathrm{pH} - \mathrm{p}K_{\mathrm{a,2}}}}{10^{\mathrm{p}K_{\mathrm{a,1}} - \mathrm{pH}} + 10^{\mathrm{pH} - \mathrm{p}K_{\mathrm{a,2}}} + 1}, \tag{7.14}$$

where $m_{\mathrm{A+}}$ and $m_{\mathrm{A-}}$ are the ionic mobilities of the fully charged cationic and anionic forms of the ampholyte A, respectively, and $\mathrm{p}K_{\mathrm{a,1}}$ and $\mathrm{p}K_{\mathrm{a,2}}$ are acidity constants of the acidic and basic groups of the ampholyte, respectively. The strong dependence of the effective mobility of this model ampholyte on the pH is shown in Figure 1.1a. For a more complex example, peptide P possessing two basic and two acidic groups, the pH dependence of its effective mobility is presented in Figure 1.1b. These two graphs demonstrate that the pH of the BGE significantly influences the effective charge and effective mobility of weak electrolytes and ampholytes and thus represents one of the main factors controlling the differences in effective mobilities of these analytes and selectivity of their electrophoretic separations. Intersection of mobility curves with the *X*-axis (pH) at the zero mobility level, that is, the pH value, at which effective charge and mobility is equal to zero, is called the isoelectric point (pI). It is an important characteristic of all amphoteric compounds. At a pH below the pI value, the ampholyte migrates in an electric field as a cation, at a pH above the pI value as an anion.

Theoretically, using the estimated values of acidity constants and ionic mobilities, the pH dependence of the effective charge and the mobility can also be obtained for polypeptides and proteins [25,26]. Nevertheless, due to the counterion adsorption (condensation) on numerous ionogenic groups of polypeptides/proteins, the real effective charge of these and other polyelectrolytes (nucleic acids, charged polysaccharides) is usually significantly lower than the calculated one [27,28].

In addition to acid–base equilibria, the effective mobility of the analyte can be also strongly influenced by its complexation with a special additive or component of the BGE. This approach is frequently utilized in the separation of enantiomers via their differently strong interactions with the chiral selectors (typically cyclodextrins or crown ethers) added into the BGE. In this case, the dependence of the effective mobility of analyte A, $m_{\mathrm{eff,A}}$, is described by the following equation [29,30]:

$$m_{\mathrm{eff,A}} = \frac{m_{\mathrm{A}} + m_{\mathrm{AC}} K_{\mathrm{b}} c_{\mathrm{C}}}{1 + K_{\mathrm{b}} c_{\mathrm{C}}}, \tag{7.15}$$

where m_{A} and m_{AC} are the ionic mobilities of the free and complexed analyte A, respectively, K_{b} is the binding constant of the complex AC, and c_{C} is the concentration of the complexing agent.

Electrophoresis when performed in the bare fused silica capillaries is frequently accompanied by another electrokinetic phenomenon, electroosmosis or electroosmotic flow (EOF). EOF is a bulk flow of the solution in the capillary caused by the application of the direct current (dc) electric field on the free

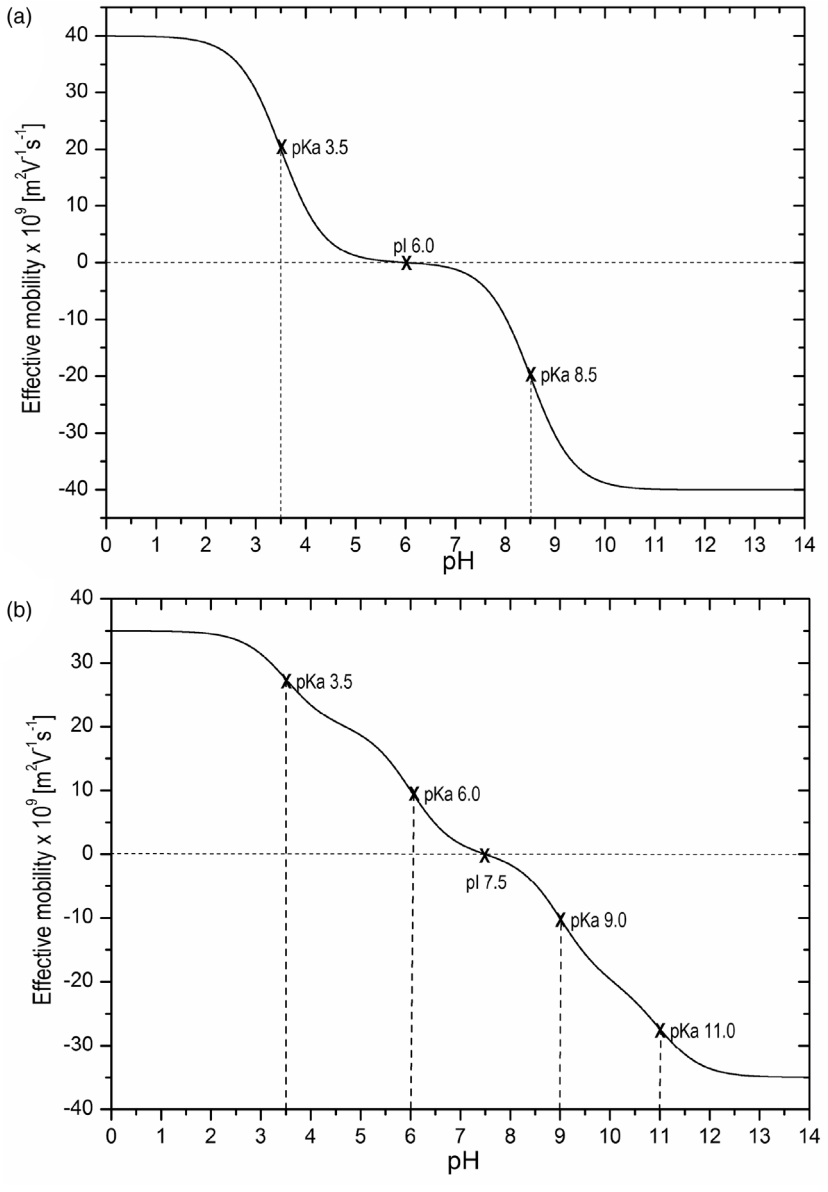

Figure 7.1 Dependence of the effective mobility of model ampholytes on pH. (a) An amino acid possessing one acidic group with pK_a 3.5 and one basic group with pK_a 8.5 and mobilities of cationic and anionic forms being $+40 \times 10^{-9}$ m^2/(V s) and -40×10^{-9} m^2/(V s), respectively. (b) A peptide possessing two acidic groups with pK_a values of 3.5 and 9.0, and two basic groups with pK_a values of 6.0 and 11.0, respectively. The ionic mobilities of dicationic and dianionic species are $+35 \times 10^{-9}$ m^2/(V s) and -35×10^{-9} m^2/(V s), respectively, and ionic mobilities of monocationic and monoanionic forms are $+20 \times 10^{-9}$ m^2/(V s), and -20×10^{-9} m^2/(V s), respectively. In both graphs, the intersection of mobility curves with the X-axis at $Y = 0$ is the isoelectric point (pI).

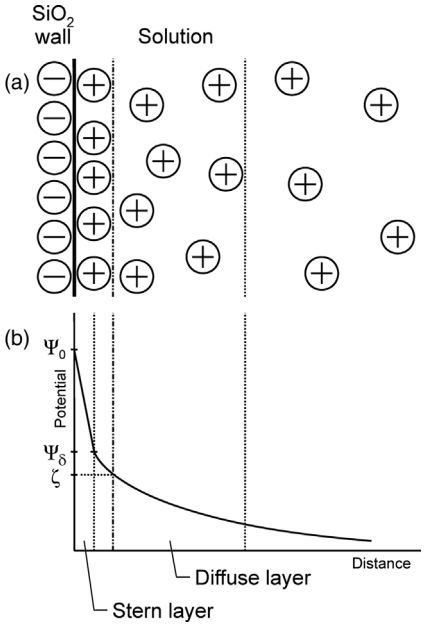

Figure 7.2 Scheme of the electric double layer at the solid–liquid interface inside the fused silica capillary (a), and course of the electric potential at this interface and inside the liquid phase (b). ψ_0 and ψ_δ are the electric potentials at the compact (Stern) region of the double layer, ζ is the electrokinetic (zeta) potential at the slipping plane between the charged surface and the electrolyte solution.

charge in the diffusion region of the electric double layer at the internal capillary wall. This double layer is generated by the dissociation of silanol groups (Si–OH) of the fused silica or by selective adsorption of one type of ions, cations, or anions, to the capillary wall, and by the free ions of the opposite charge close to the capillary wall. At a pH value above 3.0–4.0, the dissociation of silanol groups generates immobilized negative charges at the inner capillary wall; see Figure 1.2a. The cations compensating this negative charge in the diffusion region of the electric double layer create a difference of electric potential, the so-called electrokinetic potential or zeta potential, in the very thin layer (usually units to tens of nanometers) close to the capillary wall; see Figure 1.2b. When the electric field is applied inside the capillary, the hydrated cations in the diffuse region of the double layer move and together with them the whole solution inside the capillary moves due to the electric field to cathode. The strength of EOF can be characterized by its velocity, v_{eo}, or mobility, m_{eo}:

$$v_{eo} = m_{eo} E, \tag{7.16}$$

$$m_{eo} = \varepsilon_r \zeta / \eta, \tag{7.17}$$

where ζ is the electrokinetic (zeta) potential, ε_r is the relative permittivity, and η is the viscosity of the liquid medium.

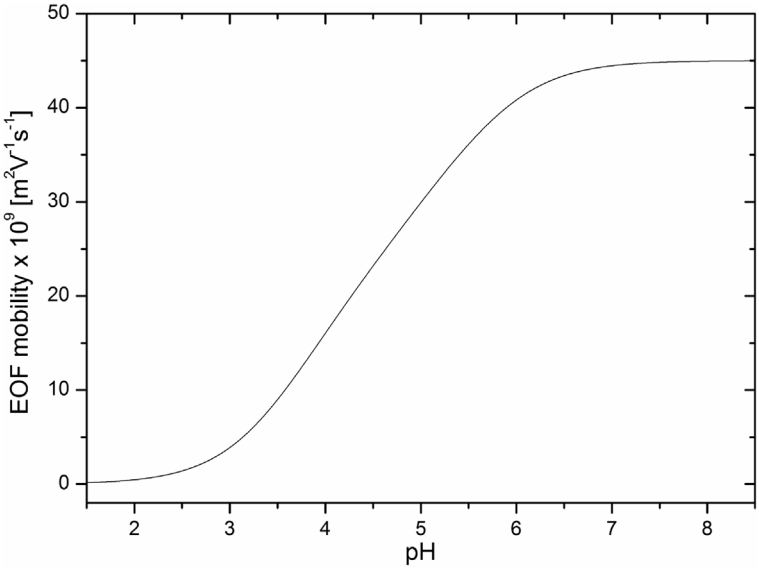

Figure 7.3 Schematic dependence of the electroosmotic flow mobility on pH in the bare fused silica capillary.

The electrokinetic potential is controlled by the surface charge density of the inner capillary wall. Since this charge is strongly dependent on the pH of the BGE inside the capillary, the EOF mobility strongly increases with increasing pH due to the increasing number of dissociated silanol groups; see Figure 1.3. The electrokinetic potential also depends on the ionic strength of the solution, as described by the Debye–Hückel theory [21]. The increased ionic strength results in constriction of the double layer, decreased zeta potential, and reduced EOF.

A unique feature of EOF is its flat "piston-like" or "plug-like" velocity profile as compared to the parabolic velocity profile of the pressure-driven hydrodynamic flow. Since the electrodriven force of the EOF is uniformly distributed at the internal walls along the capillary, there is no pressure drop inside the capillary, and the velocity is almost uniform over the whole capillary cross-section. The flat velocity profile is advantageous because it does not increase the broadening (dispersion) of zones of analytes.

7.3
Capillary Electrophoresis

7.3.1
Experimental Setup and the Separation Principle

The scheme of the basic setup of the CE device that can be also used for all other capillary electromigration techniques (CITP, CIEF, ACE, CEKC, and CEC) is shown in Figure 1.4. Heart of the system is a fused silica capillary, typically

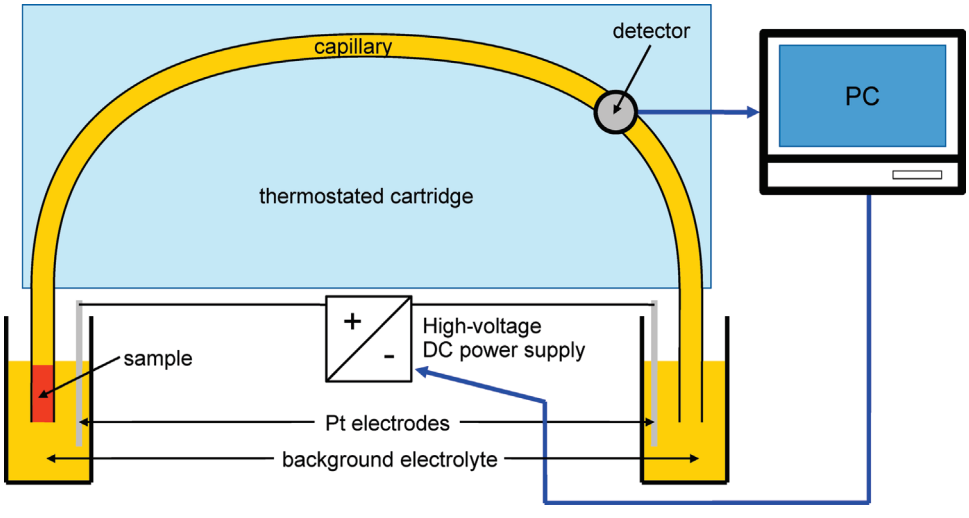

Figure 7.4 Basic setup of the device for capillary electromigration methods.

with 10–100 µm id, 150–360 µm od, 20–100 cm total length, 5–80 cm effective length (from injection end to detection point) with a 5–10 µm thin outer polyimide coating ensuring capillary mechanical stability and flexibility. The capillary is filled with the BGE (alternatively sometimes called the carrier electrolyte or the running buffer), in which the separation takes place. Both capillary ends are immersed into the electrode vessels filled with the same BGE as in the capillary. Thus, the separation is taking place in a homogeneous liquid medium. Close to the capillary outlet end, an online detector, usually the UV-spectrophotometric, fluorescence, or contactless electric conductivity type, is placed. At the beginning of the experiment, a small segment of the capillary (few mm long, i.e., of few nanoliters volume) is filled with the sample solution (see Figures 4 and 5a). The injection capillary end is placed in a sample vial and the sample solution is introduced into the capillary by pneumatically induced pressure at the injection capillary end or by vacuum pulse at the capillary outlet end or by electrokinetic injection. Once the sample is introduced into the capillary, the capillary inlet end is immersed back into the electrode vessel and a high-intensity electric field is applied to the capillary via platinum electrodes from the high-voltage power supply able to provide a separation voltage up to +30 or −30 kV and an electric current up to 300 µA. The sample components (analytes), which differ in their electrophoretic mobilities move under the influence of the applied DC electric field, with different velocities v_{ep}, to the detection (outlet) end of the capillary and on this basis they are separated.

In addition to the electrophoretic movement of the charged species, in the bare fused silica capillary, the whole bulk solution inside the capillary moves to the cathodic end of the capillary with the EOF velocity, v_{eo}. This flow, especially in neutral and alkaline BGEs, is rather strong, and EOF mobility is greater than

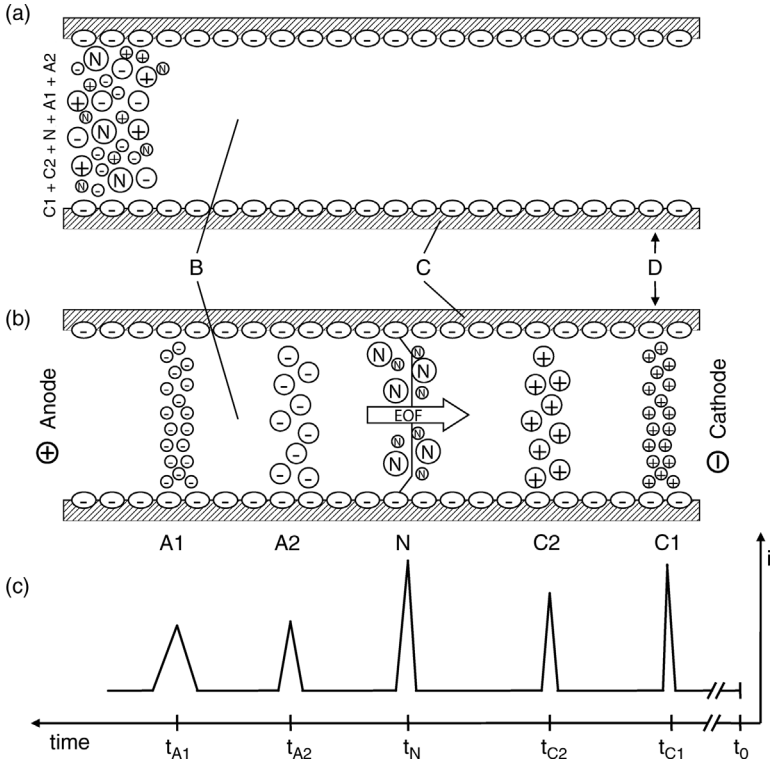

Figure 7.5 Separation principle of CE. (a) The initial state at time t_0: the sample solution containing small single-charged cations C1, large single-charged cations C2, small and large neutral compounds N, small single-charged anions A1, and large single-charged anions A2, is introduced into the capillary (C) filled with the background electrolyte (B). The electric field (voltage) is switched on. (b) The state of separation at time t_{C1}: the electric field (voltage) is being switched on and the sample components C1, C2, N, A1, and A2, differing in the charge/size ratio migrate with different resulting velocities, which are the vector sum of their electrophoretic velocities and electroosmotic flow velocity of the whole solution. The fastest component C1 passes through the detector D. (c) Schematic electropherogram: i, signal of the detector; t_{C1}, t_{C2}, t_N, t_{A2}, and t_{A1}, migration times of compounds C1, C2, N, A2, and A1, respectively.

electrophoretic mobility of both cations and anions. Hence, not only cations but also anions are transported to the cathodic capillary end and both types of ions can thus be analyzed simultaneously in one experiment (see Figure 1.5b).

The passage of the zones of the particular analytes through the detection cell is recorded by the detector, the signal of which is digitized and collected and evaluated by a computer. This computer also controls the pressure of the hydrodynamic system and the high-voltage power supply. The obtained time record of the detector signal shown in Figure 1.5c is called the electropherogram. From this record, the relevant information about quality and quantity of analytes can be derived. The qualitative parameter of the analyte is the migration time of the apex

of its peak or from this time an EOF marker migration time derived an effective electrophoretic mobility. The quantity of the analyte is directly proportional to the height or corrected area of its peak. The corrected peak area is the peak area divided by the migration time of the peak apex. This correction is necessary due to different migration velocities of the analytes through the detector.

7.3.2 Benefits of the Capillary Format

Implementation of the electrophoretic separation principle in the capillary instrumentation format had several advantages:

1) Miniaturization of the separation compartment yielding enhanced mass and volume sensitivity. Depending on the detection mode used (UV-absorption, fluorescence, mass spectrometry, conductivity, electrochemical) typically femtomoles to attomoles of analytes in a nanoliter to picoliter applied sample volume can be analyzed.
2) A stabilizing anticonvective capillary effect originating from the thin layer of the liquid inside the narrow-bore capillary tube enables separations in free liquid solutions, in which the equilibria are fast established. In addition, in the carrierless medium of the free solution CE, the risk of loss of sample components due to their adsorption to the low surface of the inner capillary wall is much less compared to liquid chromatography where the potential for a too strong or irreversible adsorption of analytes on the large surface of the stationary phase (sorbent) is rather high.
3) A relatively large ratio of capillary surface to its volume ensures efficient removal of the Joule heat, thus allowing application of high separation voltages (up to 30 kV) and high intensity of electric field (300–1000 V/cm).
4) High electric field strengths result in fast migration velocities and short analysis times (typically 5–20 min) and ensure high separation efficiencies ($10^5 - 10^7$ theoretical plates).
5) High electric resistance of the BGE placed in long capillaries with a small cross-section ensures that in spite of high voltages applied, the electric current and total electric input power (Joule heat) are rather low.
6) Relatively strong EOF allows simultaneous separation and analysis of cationic and anionic analytes in one experiment and detection of neutral components in the sample.
7) Biocompatibility. Free buffer solutions (BGEs) provide mild separation conditions preserving the biological activity of biomolecules, biopolymers, and bioparticles.
8) Using mostly small volumes (few milliliters) of aqueous solutions of the BGEs, CE is considered as a green technique, more environment- friendly than HPLC, which uses relatively large volumes of organic solvents.
9) Online detection and automation is much more user-friendly than the laborious and time-consuming staining/destaining detection procedures in the classical slab gel electrophoresis.

10) Extension of application potential. Unlike slab gel electrophoresis used mostly only for separation and analysis of biopolymers, especially proteins and nucleic acids, CE can be applied to analysis, microscale isolation, and physicochemical and biochemical characterization of all types of soluble electrically charged or ionogenic (bio)molecules and (bio)particles, independent of their size (relative molecular mass).

7.3.3 Basic Theory

The resulting migration velocity of the charged analyte, v_{mig}, in a DC electric field in the capillary is given by the sum of its effective electrophoretic velocity, v_{ep}, and EOF velocity, v_{eof}:

$$v_{mig} = v_{ep} + v_{eof} = (m_{eff} + m_{eof})E = (m_{eff} + m_{eof})U_{sep}/L_{tot}, \tag{7.18}$$

where m_{eff} is the effective electrophoretic mobility of the analyte, U_{sep} is the applied separation voltage, and L_{tot} is the total capillary length. Migration velocity v_{mig} and the EOF velocity v_{eof} can be easily determined as a ratio of the effective capillary length L_{eff} (from the injection end to the detector) and migration time of the analyte, t_{mig}, or migration time of the electroneutral EOF marker, t_{eof}, respectively:

$$v_{mig} = m_{app}E = L_{eff}/t_{mig}, \tag{7.19}$$

$$v_{eo} = m_{eo}\,E = L_{eff}/t_{eof}, \tag{7.20}$$

where m_{app} is the apparent electrophoretic mobility, and m_{eof} is the EOF mobility.

The combination of Equations 1.18, 1.19 and 1.20 gives the relation for determination of the effective electrophoretic mobility of the analyte:

$$m_{eff} = \frac{L_{eff}L_{tot}}{U_{sep}}\left(\frac{1}{t_{mig}} - \frac{1}{t_{eof}}\right). \tag{7.21}$$

The migration time, t_{mig}, that the analyte needs to migrate the distance L_{eff} is given by

$$t_{mig} = \frac{L_{eff}}{v_{mig}} = \frac{L_{eff}L_{tot}}{U_{sep}(m_{eff} + m_{eof})}. \tag{7.22}$$

If t_{mig} from Equation 1.22 is substituted into the Einstein equation for variance (σ^2) of zone length broadening due to diffusion (the only and inevitable dispersion factor under ideal conditions of CE analysis of an analyte with the diffusion coefficient D):

$$\sigma^2 = 2Dt_{mig}. \tag{7.23}$$

The following relation is obtained for the variance of the zone of analyte due to its diffusion [9]:

$$\sigma^2 = \frac{2DL_{\text{eff}}L_{\text{tot}}}{U_{\text{sep}}(m_{\text{eff}} + m_{\text{eof}})}. \tag{7.24}$$

The separation efficiency of CE can be expressed in terms of the number of theoretical plates, N, or plate height, H, defined by Equations 1.25 and 1.26 [31]:

$$N = L_{\text{eff}}^2/\sigma^2. \tag{7.25}$$

$$H = L_{\text{eff}}/N. \tag{7.26}$$

Substituting Equations 1.24 into 1.25 and Equation 1.25 into Equation 1.26 results in the following relations for N and H in CE, respectively:

$$N = \frac{L_{\text{eff}}E(m_{\text{eff}} + m_{\text{eof}})}{2D}. \tag{7.27}$$

$$H = \frac{L_{\text{eff}}}{N} = \frac{2D}{E(m_{\text{eff}} + m_{\text{eof}})}. \tag{7.28}$$

From Equations 1.22, 1.24, 1.27, and 1.28, the reason for advantageous application of a high electric field strength (separation voltage) in CE is obvious: the separation efficiency increases (variance, plate height, and time decrease) with increasing electric field strength or separation voltage for the given capillary length. Of course, the voltage can be increased only to levels under which the temperature gradients inside the capillary remain reasonably low. Usually, the electric input power (product of voltage and current) is less than 5 W per 1 m of capillary length. These equations also show that the higher separation efficiency (lower plate height) can be achieved for analytes with high mobility (small ions with high charge) or with low diffusion coefficient (macroions) than for low mobility analytes ((macro)ions with low charge) or analytes with high diffusion coefficients (small ions).

The theoretical plate number for the particular analyte can be determined from an electropherogram using the following equation [31]:

$$N = 5.54\left(\frac{t}{w_{1/2}}\right)^2, \tag{7.29}$$

where t is the migration time of the analyte and $w_{1/2}$ is its peak width at half height.

For practical separation purposes, more than the number of theoretical plates, the real separation of sample components is important. The separation of the two components is characterized by a resolution of their peaks, R_s, defined as [31]:

$$R_S = \frac{2(t_2 - t_1)}{w_1 + w_2}, \tag{7.30}$$

where t_2 and t_1 are the migration times of the two analytes, and w_1 and w_2 are the baseline widths of their peaks. In Gaussian peaks, for the baseline peak width w_b the following relation holds:

$$w_b = 4\sigma, \tag{7.31}$$

where σ is the standard deviation of the peak in time, length, or volume units.

For the resolution R_s, which is a quantitative parameter of the selectivity of the method, the following relation can be derived [32]:

$$R_s = \frac{\sqrt{N}}{4}\frac{\Delta m}{m_{av}} = \frac{\Delta m}{4\sqrt{2}}\left(\frac{U_{sep}}{D(m_{av} + m_{eof})}\right)^{1/2}, \tag{7.32}$$

where Δm is the mobility difference between two analytes ($\Delta m = m_2 - m_1$) and m_{av} is their average mobility ($m_{av} = (m_1 + m_2)/2$).

Equation 1.32 shows that for the resolution, that is, for selectivity of the method, the difference in mobilities is more important than the separation efficiency since resolution increases linearly with the mobility difference but only with the square root of the separation efficiency and voltage. Equation 1.32 also indicates that infinite resolution can be obtained when the absolute values of m_{av} and m_{eof} are almost equal but have opposite signs, that is, if $|m_{eff} + m_{eof}|$ is close to zero. However, in this case, the analysis time is close to infinity. Hence, in practice, the separation parameters have to be compromised to achieve both reasonable resolution and separation time.

7.3.4 Dispersion Effects in CE

As shown above, separation of analytes by CE is based on the differences in their effective electrophoretic mobilities. However, for a successful CE separation of two compounds not only the difference of their mobilities but also the minimal dispersion (broadening) of their migrating zones is extremely important. Variance of the analyte zone in CE as expressed by Equation 1.24 takes into account only the diffusion of the analyte, which is an inevitable phenomenon, and minimal dispersion effect in CE and represents ideal conditions for CE separation. In real CE experiments, several other dispersion effects occur and the total variance of the analyte zone in CE is equal to the sum of several particular variances [33,34]:

$$\sigma^2 = \sigma^2_{dif} + \sigma^2_{temp} + \sigma^2_{elm} + \sigma^2_{eof} + \sigma^2_{lmf} + \sigma^2_{ads} + \sigma^2_{inj} + \sigma^2_{det} + \sigma^2_{coil} + \ldots, \tag{7.32}$$

where the subscripts refer to diffusion, temperature gradients due to Joule heating, electromigration dispersion, EOF, imposed hydrodynamic laminar flow, adsorption of analyte to capillary wall, length of the sample injection zone, length of the detection cell, and capillary coiling, respectively.

7.3.4.1 Diffusion

Longitudinal and radial diffusion, that is, the spontaneous motion of an analyte due to a gradient of its concentration (chemical potential) in axial and radial directions inside the capillary is an inevitable dispersion effect in CE. Total zone broadening can be never smaller than the dispersion caused by diffusion. Because of the flat "piston-like" velocity profile of EOF and a very narrow diffusion region of the electric double layer (usually units to tens of nanometers) at the capillary wall, the influence of radial diffusion on the zone broadening can be neglected. The effect of longitudinal diffusion in CE leading to symmetrical zone broadening with the Gaussian concentration profile was described in Section 1.3.3. From this description it follows that the dispersion due to diffusion can be minimized by reduction of migration time, that is, by increasing the voltage and/or decreasing the capillary length.

7.3.4.2 Temperature Gradients Due to Joule Heating

Passage of an electric current through the capillary generates Joule heat. Joule heat per unit time is equal to the product of current and voltage (input power). In CE, the usual input power per unit capillary length is in the range 0.5–5.0 W/m and may cause the temperature to increase up to several tens of degrees of Celsius depending on the way of capillary cooling or thermostatization (active or passive, liquid or air) [35–37]. The absolute increase of temperature need not be always harmful, but the radial and longitudinal temperature gradients can significantly reduce the separation efficiency. The radial temperature gradient is caused by a worse heat dissipation in the center of the capillary than at its inner wall. Longitudinal gradients originate from different heat dissipations occurring along the capillary (thermostated vs. nonthermostated capillary sections) [38]. These gradients cause viscosity differences in the BGE and hence mobility differences in different capillary parts and lead to zone deformation and broadening. Control of temperature is important since one degree change in temperature results in 2–2.5% change in viscosity and mobility. An average increase of temperature inside the capillary can be measured from the changes in resistance of a strong electrolyte of known specific electric conductivity (e.g., 20 mM KCl) on increasing the input power [39].

The negative effect of Joule heating becomes obvious when an increase of voltage (electric field strength), theoretically leading to the higher separation efficiency – see Equation 1.27, results in reduction of separation efficiency. The safe region of voltage can be derived from Ohm's plot (current vs. voltage). Increase of temperature inside the capillary can be neglected if this plot is linear, which indicates a constant electric resistance and temperature inside the capillary. The Joule heating effect can be reduced by decreasing the input power, capillary inner diameter, and conductivity (concentration, ionic strength) of the BGE and using active capillary cooling by circulating liquid or gaseous media.

7.3.4.3 Electromigration Dispersion

Electromigration dispersion leads to asymmetrical triangular-like zone broadening. It is a consequence of differences in electric conductivity and electric field intensity in the zone of the analyte and in the surrounding BGE. Two cases can occur. In the first case, the effective mobility of the analyte ion is greater than that of the BGE coion (= BGE ion of the same sign as the analyte ion). Then the conductivity of this zone is higher and the intensity of the electric field is lower than that in the BGE. Hence, if the analyte ion at the front boundary of its zone enters the zone of BGE, where the electric field is stronger, its velocity is increased and results in broadening of the front portion of its zone, that is, the zone is fronting. The back boundary of the analyte zone remains approximately the same because if the analyte ion enters the BGE, it will be accelerated by the higher electric field and will return to its zone whereas the BGE coion entering the analyte zone will be decelerated by the lower electric field in this zone and will return back into the BGE zone. In the second case, the situation is reverse. The effective mobility of the analyte is lower than that of the BGE coion. Then the conductivity of this zone is lower and the intensity of the electric field is higher than that in the BGE. Hence, if the analyte ion crosses the back boundary of its zone and enters the zone of BGE, where the electric field is lower, its velocity is decreased and results in broadening of the back portion of its zone, that is, the zone is tailing. The front boundary of the analyte zone remains approximately the same because if analyte ion enters the BGE, it will be decelerated by the lower electric field and will return to its zone whereas the BGE coion entering the analyte zone will be accelerated by the higher electric field in this zone and will return to the BGE zone. A detailed theoretical description can be found in specialized papers [40,41]. From a practical point of view it is important that electromigration dispersion significantly decreases with the increasing ratio of BGE coion concentration versus analyte ion concentration and becomes negligible if the analyte concentration is two to three orders lower than that of the BGE coion.

Recently, a special type of electromigration dispersion due to complexation reaction was discovered in the system containing a neutral complex-forming agent (native or methylated β-cyclodextrin) and a fully charged analyte (*R*-flurbiprofen) [42].

7.3.4.4 Dispersion due to EOF

Analyte zone dispersion due to EOF in an open capillary with homogeneous electrokinetic potential along the capillary wall is rather small because of the "piston-like" velocity profile with usually a very thin diffuse region of the electric double layer (an analog to the Debye length of the ionic atmosphere of the ion) at the capillary wall. This layer is not moving, thus contributing to the partial zone dispersion. Usually, the thickness of this layer (units to tens of nanometers) is much less than the capillary diameter (25–75 μm) and in this case the following relation was derived for peak broadening due to the radial EOF profile [43]:

$$H_{\mathrm{eof}} = \beta^2 \nu_{\mathrm{eof}} / D, \tag{7.34}$$

where β is the thickness of the diffusion layer, v_{eof} is the velocity of EOF, and D is the diffusion coefficient of the analyte. However, the contribution of EOF to the total dispersion may become significant for very large analytes with a low diffusion coefficient and in the capillaries with a nonuniform zeta potential distribution along the wall [44]. In the latter case, the turbulences can occur at the boundary of capillary sections with a stepwise change of electrokinetic potential. Hence, uniformly coated or uncoated capillaries should be used for high-efficiency CE separations.

7.3.4.5 Imposed Hydrodynamic Laminar Flow

Imposed hydrodynamic laminar flow occurs in the CE if there is a height difference of BGE solutions in the electrode vessels or in the so-called pressure-assisted CE [45,46], when the separation is accelerated or decelerated by pressure-driven flow downstream or upstream of EOF or the electrophoretic migration of analytes. The Taylor dispersion due to the parabolic profile of this flow is characterized by the dispersion coefficient K_{lf}, which can be calculated from Equation 1.35 [47]:

$$K_{lf} = \frac{r_c^2 (2v_f)^2}{192D}, \tag{7.35}$$

where r_c is the capillary radius, v_f is the average flow velocity, and D is the diffusion coefficient. Additivity of dispersion by longitudinal molecular diffusion and the parabolic profile of the laminar flow allows to sum K_{lf} and D for the total dispersion.

7.3.4.6 Analyte Adsorption to the Capillary Wall

Another negative effect lowering the separation efficiency and resolution of CE is the adsorption of analytes on the inner capillary wall. Depending on the strength and kinetics of the analyte–wall interactions, small or large peak tailing, reduced analyte recovery, or even a total analyte sorption and loss of sample may occur. The ionic interactions between cationic analytes and negatively charged dissociated silanol groups of the fused silica capillary as well as hydrophobic and hydrophilic interactions between analytes and fused silica represent the main forces responsible for analyte adsorption on the capillary wall. The adsorption effects cause serious problems especially in CE analyses of proteins and polypeptides, since these amphoteric substances possess both cationic and anionic ionogenic groups and hydrophobic and hydrophilic moieties.

These interactions can be described using the chromatographic concept of theoretical plate height. If a slow linear adsorption of analytes takes place at the inner capillary wall, for the plate height contribution due to adsorption, H_{ads}, the following equation was derived [32]:

$$H_{ads} = \left[\frac{K^2}{D}\frac{r_c}{r_c + 2K} + \frac{4K}{(r_c + 2K)k_d}\right] v_{mig}, \tag{7.36}$$

where K is the distribution coefficient defined as the ratio of analyte equilibrium concentration in the solid surface (stationary phase) and liquid solution (liquid phase), D is the diffusion coefficient, r_c is the inner capillary radius, k_d is the rate constant of desorption, and v_{mig} is the migration velocity. The two terms in the brackets of this equation indicate that both radial diffusion and kinetics of sorption/desorption contribute to the dispersion of the analyte peak. Equation 1.36 also shows that plate height contribution due to wall adsorption increases with increasing migration velocity, that is, with increasing electric field strength, analyte mobility, and EOF mobility (if both these mobilities have the same sign or one of them is dominant).

Suppression of Adsorption and Regulation of EOF

Adsorption causes substantial reduction of CE separation power and/or loss of analyzed compounds. Thus, suppression of adsorption is still a great challenge in CE. There are several strategies to suppress the adsorption of analytes on the inner capillary walls.

The simplest way is to use either (i) very acidic BGEs (pH < 2), in which the dissociation of silanol groups is suppressed and electrostatic interactions with positively charged analytes are reduced, or (ii) alkaline BGE at pH 8–11, at which silanol groups are fully dissociated and their negative charges repulse the anionic analytes, or (iii) high ionic strength BGEs, in which the high concentration of ions in the BGE ensures that they preferentially occupy the active charged group in the capillary wall and prevents their interactions with analytes. For example, the pH of the BGE for CE analysis of proteins and peptides should be at least two pH units above their isoelectric points resulting in electrostatic repulsion of negatively charged protein/peptide molecules and negative charge of dissociated silanol groups on the inner wall of the fused silica capillary. Nevertheless, application of this approach is relatively limited due to chemical instability of proteins/peptides at a high pH.

The most common approach is to modify the inner capillary wall using variable coatings. The coatings can be classified into three categories.

1) Dynamic coatings are based on reversible (dynamic) adsorption of small ions, for example, small amines and oligoamines, anionic and cationic surfactants (sodium dodecyl sulfate (SDS) or cetyltrimethylammonium bromide (CTAB) at subcritical micellar concentration level), and amphoteric compounds (betain) or hydrophilic polymers (cellulose derivatives or polysaccharides) on the capillary wall [48–50]. Dynamic coatings are simply added to the BGE, which makes their use very easy but on the other hand they need not be always well compatible with suitable separation conditions and detection; for example, UV-absorbing compounds interfere with UV-absorption detection and many compounds can be barely used in CE with electrospray ionization mass spectrometry (ESI-MS) detection because of signal suppression or contamination of the ion source. Amines and cationic detergents create positively charged capillary coatings suitable

for separation of cationic analytes, the sorption of which is minimized by electrostatic repulsion. Analogously, sorption of anionic analytes is reduced by their repulsion from negatively charged coatings of anionic detergents.

2) Covalently bound coatings are coupled to the fused silica surface by chemical reaction with the activated silanol groups. They are implemented by attachment of polymers to the capillary wall via bifunctional agents reacting in the first step with the capillary wall and in the second step with the functional group of the polymer. Covalent coatings of fused silica capillaries with variable polymers (natural, synthetic, neutral, cationic, anionic, hydrophilic, hydrophobic, linear, grafted, or cross-linked), such as linear and grafted cellulose derivatives, poly(vinylalcohol), poly(oxyethylene), linear and cross-linked poly(acrylamide) and its derivatives, and linear and cross-linked poly(ethyleneimine) were found to be effective in suppressing peptides and proteins' adsorption and enhancing the separation efficiency of their CE separations [49,51]. Unlike dynamic coatings, they can be very stable, may provide suitable surface properties and a good compatibility with ESI-MS detection. However, covalent coatings also have disadvantages: some coating procedures are rather complicated, laborious, time-consuming, and expensive. Recoating steps (e.g., in the case of strong adsorption of the analytes to the coating material) is not possible.
3) Physically adsorbed coatings are a compromise between dynamic and covalently bound coatings. Variable polymers with a relatively high molecular mass and thus strong physical adsorption properties are used for this purpose, for example, several types of neutral polymers (cellulose derivatives, poly(vinylalcohol), poly(ethylene oxide), poly(vinylpyrrolidone), poly(dimethylacrylamide) homo- and copolymers of acrylamide), polymeric surfactants (polyoxyethylene ether – Brij-35); anionic polymers (dextran sulfate, poly(vinyl sulfonic acid); and cationic polymers (hexadimethrine bromide (polybrene), poly(ethyleneimine), poly(diallyldimethylammonium) chloride, and *N*-methylpolyvinylpyridinium) [50]. These coatings are simply created by rinsing the capillary with a polymer solution before the CE analyses. They are rather stable under common CE conditions, there is no need to add them to the BGE and hence they are compatible with MS detection. In contrast to covalently attached polymers, the physically adsorbed coatings can be easily refreshed by repeating the coating procedure, thus increasing the total lifetime of the coated capillaries and making them more suitable for the analysis of matrix-afflicted samples. However, coating stability can be significantly reduced in strongly alkaline BGEs and/or by a high content of the organic solvent in the BGE.

Some cationic polymers, such as polybrene, poly(ethyleneimine), and poly(diallyldimethylammonium) chloride have been employed as cationic noncovalent coatings providing high EOF and repulsion of cationic analytes (e.g., proteins and peptides below their isoelectric point, pI) from the capillary wall,

thus yielding a high separation efficiency. A stable wall modification was accomplished by creating successive multiple ionic polymer layers (SMIL technology) [52,53]. Bilayers, triple layers, or even multiple layers can be formed by polymers of opposite charge being alternatively adsorbed on each other. Bilayer coatings consisting of polybrene-poly(vinyl sulfonic acid) or triple layers of polybrene–dextran sulfate–polybrene substantially reduced the adsorption of protein and peptides in their CE-MS analysis.

Dynamic or permanent capillary coatings have been also used for control of the EOF, which influences separation efficiency, resolution, and speed of CE analyses [54]. A high and repeatable anodic or cathodic EOF for CE-MS separation of peptides was achieved by noncovalent coating of the fused silica capillary with single or multiple layers of polycationic polybrene or polycationic polybrene/polyanionic dextrane sulfate [52,53].

7.3.4.7 Length of the Sample Injection Zone

To prevent the additional zone broadening due to the injection, the injection length of the sample zone should be smaller than the diffusion-caused zone dispersion, that is, the sample zone should be rather short. However, for detection reasons, the zone length of diluted samples has to be frequently larger. Then the zone dispersion due to injection depends on the manner of sample introduction. For the electrokinetic (electrophoretic and/or electroosmotic) injection with the rectangular concentration distribution of the sample plug of the length L_S, the corresponding plate height contribution, $H_{inj,ek}$ is [32]

$$H_{inj,ek} = L_S^2/12L_{eff}. \tag{7.37}$$

Length L_S can be calculated from the electrophoretic and electroosmotic velocities during sample injection and injection time.

For the pressure-driven hydrodynamic sample injection with a parabolic flow profile and nonrectangular concentration distribution, the expression for the plate height contribution due to hydrodynamic injection, $H_{inj,hd}$ is more complicated [32]:

$$H_{inj,hd} = \frac{r_c^6 \Delta P^2 t_{inj}}{1536 L_{tot}^2 \eta^2 D L_{eff}}. \tag{7.38}$$

This equation, where r_c is the capillary inner radius, ΔP is the injection pressure, and t_{inj} is the injection time, shows that in this case, the plate height contribution due to injection very strongly increases with capillary radius.

Independent of the sample-injection mode, for high-efficiency CE separation, the sample injection zone should be as narrow as possible. A narrow starting zone can be achieved by variable concentrating effects employed in CE, such as field-amplified sample stacking (the analyte is concentrated due to higher electric field strength in the zone of the sample dissolved in water or in diluted BGE than in the BGE), field-enhanced (amplified) sample injection (the analyte is injected electrokinetically from the diluted sample solution in the absence or

presence of pressure), sweeping (the analyte is concentrated in the micellar zone), dynamic pH junction (the analyte is concentrated in the zone with a stepwise changed pH), and isotachophoretic or transient isotachophoretic stacking (the analyte is concentrated due to the concentrating effect of the discontinuous ITP electrolyte system) [55].

7.3.4.8 Length of Detection Cell

The on-column detection cell of the most frequently used UV-absorption detector is usually of a rectangular shape, hence plate height contribution due to the detection cell (aperture) length (L_{det}), H_{det}, is identical to plate height contribution due to rectangular sample injection [32]:

$$H_{det} = L_{det}^2/12L_{eff}. \tag{7.39}$$

L_{det} is usually very narrow, so in practice the H_{det} is mostly negligible compared to other plate height contributions.

7.3.4.9 Capillary Coiling

In the coiled capillaries placed in the limited volume cartridges, the zone broadening occurs due to different lengths of the trajectories of analyte particles moving at the inner and outer circumference of the capillary coil. This difference in length of the migration paths results in the plate height contribution due to the capillary coiling, H_{coil}, [56]:

$$H_{coil} = r_c^2 L_{eff}/4R_{coil}^2, \tag{7.40}$$

where R_{coil} is the internal radius of the capillary coil.

The effect of capillary coiling on peak broadening can be significant if very large analytes with low diffusion coefficients are separated and/or if capillaries with small coil radii are used, for example, narrow coiled microchannels on the microchips.

7.4 Conclusions

During the past three decades, CE has developed into a high-performance separation method with extremely high application potential. In principle, CE can be used for analysis and/or micropreparative separation of any soluble ionogenic compounds, both low and high molecular mass substances and particles, for example, organic and inorganic acids and bases, metal ions, mono-, oligo-, and polysaccharides, amino acids, peptides, proteins, nucleosides, mono-, oligo-, and polynucleotides, nucleic acids, synthetic polymers, and (bio)particles, such as organic and inorganic nanoparticles, viruses, bacteria, cells, and organelles. According to the sample character and according to the purpose of the analysis, four classes of applications can be distinguished:

- Purity control including enantiopurity control of both naturally occurring and synthetic compounds, that is, quality control of chemicals, drugs, dyes, explosives, toxins, environmental pollutants, vitamins, enzymes, hormones, antibodies, and so on.
- *Analysis of complex mixtures*: Determination of biologically and/or chemically important analytes, for example, metabolites, drugs, vitamins, hormones, additives, and pollutants in biological fluids (serum, plasma, CSF, urine, saliva, and sweat), tissue extracts, food products, drinks, and waste waters.
- *Monitoring of chemical and biological conversions*: Chemical and enzymatic reactions, metabolite and drug conversions, analyte interactions, and so on.
- *Physicochemical characterization of the above types of analytes*: Determination of effective and absolute electrophoretic mobilities, isoelectric points, relative molecular masses, Stokes radii, diffusion coefficients, acid dissociation constants of their ionogenic groups, stability constants of their complexes with both low and high molecular mass ligands and rate constants of their chemical reactions and enzymatic conversions.

To summarize, CE is a powerful tool in all areas, where the above given analytical and separation problems are solved: chemistry, biochemistry, molecular biology, pharmacy, medicine, food and feed industry, agriculture, environmental analysis, energetic, and so on.

Acknowledgments

This work was supported by the Czech Science Foundation, grant nos. P206/12/0453 and 13–17 224 S, and by the Academy of Sciences of the Czech Republic, Research Project RVO 61 388 963. M. Růžička and P. Sázelová are thanked for their technical assistance.

References

1 Righetti, P.G. (2005) Electrophoresis: The march of pennies, the march of dimes. *J. Chromatogr. A*, **1079** (1–2), 24–40.
2 Hruška, V. and Gaš, B. (2007) Kohlrausch regulating function and other conservation laws in electrophoresis. *Electrophoresis*, **28** (1–2), 3–14.
3 Gaš, B. (2009) Theory of electrophoresis: Fate of one equation. *Electrophoresis*, **30**, S7–S15.
4 Tiselius, A. (1937) A new apparatus for electrophoretic analysis of colloidal mixtures. *Trans. Faraday Soc.*, **33**, 524–531.
5 Hjertén, S. (1967) Free zone electrophoresis. *Chromatogr. Rev.*, **9** (2), 122–219.
6 Virtanen, R. (1974) Zone electrophoresis in a narrow-bore tube employing potentiometric detection: theoretical and experimental study. *Acta Polytech. Sc. Ch.*, (123), 1–67.
7 Everaerts, F.M., Beckers, J.L., and Verheggen, T.P.E.M. (1976) *Isotachophoresis: Theory, Instrumentation and Applications*, Elsevier, Amsterdam.
8 Everaerts, F.M., Geurts, M., Mikkers, F.E.P., and Verheggen, T.P.E.M. (1976)

Analytical isotachophoresis. *J. Chromatogr.*, **119**, 129–155.
9 Jorgenson, J.W. and Lukacs, K.D. (1981) Zone electrophoresis in open-tubular glass-capillaries. *Anal. Chem.*, **53** (8), 1298–1302.
10 Jorgenson, J.W. and Lukacs, K.D. (1983) Capillary zone electrophoresis. *Science*, **222** (4621), 266–272.
11 Grossman, P.D. and Colburn, J.C. (1992) *Capillary Electrophoresis: Theory and Practice* (eds P.D. Grossman and J.C. Colburn), Academic Press, Inc., San Diego.
12 Foret, F., Křivánková, L., and Boček, P. (1993) *Capillary Zone Electrophoresis*, Verlag Chemie, Weinheim.
13 Khaledi, M.G. (ed.) (1998) *High-Performance Capillary Electrophoresis: Theory, Techniques, and Applications*, John Willey & Sons, Inc., New York.
14 Landers, J.P. (ed.) (2008) *Handbook of Capillary and Microchip Electrophoresis and Associated Microtechnics*, 3rd edn., CRC Press, Taylor & Francis Group, Boca Raton.
15 Schmitt-Kopplin, P. (ed.) (2008) *Capillary Electrophoresis: Methods and Protocols*, Humana Press, Munchen, Germany.
16 Lauer, H.H. and Rozing, G.P. (2009) High Performance Capillary Electrophoresis. A primer, Agilent Technologies, Waldbronn.
17 Volpi, N. and Maccari, F. (2013) *Capillary Electrophoresis of Biomolecules. Methods and Protocols*, 1st edn, Humana Press, Springer, New York, Heidelberg, Dordrecht, London.
18 Garcia, C.D., Chumbimuni-Torres, K.Y., and Carrilho, E. (2013) *Capillary Electrophoresis and Microchip Capillary Electrophoresis: Principles, Applications, and Limitations*, John Wiley & Sons, Inc., Hoboken, New Jersey.
19 Frost, N.W., Jing, M., and Bowser, M.T. (2010) Capillary electrophoresis. *Anal. Chem.*, **82** (12), 4682–4698.
20 Geiger, M., Hogerton, A.L., and Bowser, M.T. (2012) Capillary electrophoresis. *Anal. Chem.*, **84** (2), 577–596.
21 Koval, D., Kašička, V., and Zusková, I. (2005) Investigation of the effect of ionic strength of Tris-acetate background electrolyte on electrophoretic mobilities of mono-, di-, and trivalent organic anions by capillary electrophoresis. *Electrophoresis*, **26** (17), 3221–3231.
22 Jaroš, M., Včeláková, K., Zusková, I., and Gaš, B. (2002) Optimization of background electrolytes for capillary electrophoresis: II. Computer simulation and comparison with experiments. *Electrophoresis*, **23** (16), 2667–2677.
23 Koval, D., Kašička, V., Jiráček, J., Collinsova, M., and Garrow, T.A. (2002) Analysis and characterization of phosphinic pseudopeptides by capillary zone electrophoresis. *Electrophoresis*, **23** (2), 215–222.
24 Šolínová, V. and Kašička, V. (2013) Determination of acidity constants and ionic mobilities of polyprotic peptide hormones by CZE. *Electrophoresis*, **34** (18), 2655–2665.
25 Kašička, V. and Prusík, Z. (1989) Isotachophoretic analysis of peptides. Selection of electrolyte systems and determination of purity. *J. Chromatogr. A*, **470** (1), 209–221.
26 Mosher, R.A., Gebauer, P., and Thormann, W. (1993) Computer simulation and experimental validation of the electrophoretic behavior of proteins 3. Use of titration data predicted by the protein's amino acid composition. *J. Chromatogr. A*, **638** (2), 155–164.
27 Ibrahim, A., Koval, D., Kašička, V., Faye, C., and Cottet, H. (2013) Effective charge determination of dendrigraft poly-L-lysine by capillary isotachophoresis. *Macromolecules*, **46** (2), 533–540.
28 Chamieh, J., Koval, D., Besson, A., Kašička, V., and Cottet, H. (2014) Generalized polymer effective charge measurement by capillary isotachophoresis. *J. Chromatogr. A*, **1370**, 255–262.
29 Hruška, V., Beneš, M., Svobodová, J., Zusková, I., and Gaš, B. (2012) Simulation of the effects of complex-formation equilibria in electrophoresis: I. Mathematical model. *Electrophoresis*, **33** (6), 938–947.
30 Svobodová, J., Beneš, M., Hruška, V., Ušelová, K., and Gaš, B. (2012) Simulation of the effects of complex-formation equilibria in electrophoresis: II. Experimental verification. *Electrophoresis*, **33** (6), 948–957.

31 Ettre, L.S. (1993) Nomenclature for chromatography. *Pure Appl. Chem.*, **65** (4), 819–872.

32 Kenndler, E. (1998) Theory of capillary zone electrophoresis, in *High-Performance Capillary Electrophoresis: Theory, Techniques, and Applications* (ed. M.G. Khaledi), John Willey & Sons, Inc., New York, pp. 25–76.

33 Gaš, B. and Kenndler, E. (2000) Dispersive phenomena in electromigration separation methods. *Electrophoresis*, **21** (18), 3888–3897.

34 Datta, S. and Ghosal, S. (2009) Characterizing dispersion in microfluidic channels. *Lab. Chip.*, **9** (17), 2537–2550.

35 Evenhuis, C.J. and Haddad, P.R. (2009) Joule heating effects and the experimental determination of temperature during CE. *Electrophoresis*, **30** (5), 897–909.

36 Evenhuis, C.J., Musheev, M.U., and Krylov, S.N. (2011) Universal method for determining electrolyte temperatures in capillary electrophoresis. *Anal. Chem.*, **83** (5), 1808–1814.

37 Patel, K.H., Evenhuis, C.J., Cherney, L.T., and Krylov, S.N. (2012) Simplified universal method for determining electrolyte temperatures in a capillary electrophoresis instrument with forced-air cooling. *Electrophoresis*, **33** (6), 1079–1085.

38 Musheev, M.U., Filiptsev, Y., and Krylov, S.N. (2010) Temperature difference between the cooled and the noncooled parts of an electrolyte in capillary electrophoresis. *Anal. Chem.*, **82** (20), 8692–8695.

39 Koval, D., Kašička, V., Jiráček, J., Collinsova, M., and Garrow, T.A. (2002) Determination of dissociation constant of phosphinate group in phosphinic pseudopeptides by capillary zone electrophoresis. *J. Chromatogr. B*, **770** (1–2), 145–154.

40 Hruška, V., Riesová, M., and Gaš, B. (2012) A nonlinear electrophoretic model for PeakMaster: I. Mathematical model. *Electrophoresis*, **33** (6), 923–930.

41 Riesová, M., Hruška, V., and Gaš, B. (2012) A nonlinear electrophoretic model for PeakMaster: II. Experimental verification. *Electrophoresis*, **33** (6), 931–937.

42 Beneš, M., Svobodová, J., Hruška, V., Dvořák, M., Zusková, I., and Gaš, B. (2012) A nonlinear electrophoretic model for PeakMaster: Part IV. Electromigration dispersion in systems that contain a neutral complex-forming agent and a fully charged analyte. Experimental verification. *J. Chromatogr. A*, **1267**, 109–115.

43 Gaš, B., Štědrý, M., and Kenndler, E. (1995) Contribution of the electroosmotic flow to peak broadening in capillary zone electrophoresis with uniform zeta potential. *J. Chromatogr. A*, **709** (1), 63–68.

44 Potoček, B., Gaš, B., Kenndler, E., and Štědrý, M. (1995) Electroosmosis in capillary zone electrophoresis with non-uniform zeta potential. *J. Chromatogr. A*, **709** (1), 51–62.

45 Zinellu, A., Sotgia, S., Scanu, B., Pisanu, E., Sanna, M., Usai, M.F., Deiana, L., and Carru, C. (2010) Ultra-fast adenosine 5′-triphosphate, adenosine 5′-diphosphate and adenosine 5′-monophosphate detection by pressure-assisted capillary electrophoresis UV detection. *Electrophoresis*, **31** (16), 2854–2857.

46 Mai, T.D. and Hauser, P.C. (2013) Study on the interrelated effects of capillary diameter, background electrolyte concentration, and flow rate in pressure assisted capillary electrophoresis with contactless conductivity detection. *Electrophoresis*, **34** (12), 1796–1803.

47 Sonke, J.E., Furbish, D.J., and Salters, V.J.M. (2003) Dispersion effects of laminar flow and spray chamber volume in capillary electrophoresis–inductively coupled plasma–mass spectrometry: a numerical and experimental approach. *J. Chromatogr. A*, **1015** (1–2), 205–218.

48 Righetti, P.G., Gelfi, C., Verzola, B., and Castelletti, L. (2001) The state of the art of dynamic coatings. *Electrophoresis*, **22** (4), 603–611.

49 Horvath, J. and Dolnik, V. (2001) Polymer wall coatings for capillary electrophoresis. *Electrophoresis*, **22** (4), 644–655.

50 Lucy, C.A., MacDonald, A.M., and Gulcev, M.D. (2008) Non-covalent capillary coatings for protein separations in capillary electrophoresis. *J. Chromatogr. A*, **1184** (1–2), 81–105.

51 Huhn, C., Ramautar, R., Wuhrer, M., and Somsen, G.W. (2010) Relevance and use of capillary coatings in capillary electrophoresis–mass spectrometry. *Anal. Bioanal. Chem.*, **396** (1), 297–314.

52 Haselberg, R., Brinks, V., Hawe, A., de Jong, G.J., and Somsen, G. (2011) Capillary electrophoresis–mass spectrometry using noncovalently coated capillaries for the analysis of biopharmaceuticals. *Anal. Bioanal. Chem.*, **400** (1), 295–303.

53 Nehme, R., Perrin, C., Cottet, H., Blanchin, M.D., and Fabre, H. (2011) Stability of capillaries coated with highly charged polyelectrolyte monolayers and multilayers under various analytical conditions: application to protein analysis. *J. Chromatogr. A*, **1218** (22), 3537–3544.

54 Sola, L. and Chiari, M. (2012) Modulation of electroosmotic flow in capillary electrophoresis using functional polymer coatings. *J. Chromatogr. A*, **1270**, 324–329.

55 Breadmore, M.C., Shallan, A.I., Rabanes, H.R., Gstoettenmayr, D., Keyon, A.S.A., Gaspar, A., Dawod, M., and Quirino, J.P. (2013) Recent advances in enhancing the sensitivity of electrophoresis and electrochromatography in capillaries and microchips (2010–2012) *Electrophoresis*, **34** (1), 29–54.

56 Kašička, V., Prusík, Z., Gaš, B., and Štědrý, M. (1995) Contribution of capillary coiling to zone dispersion in capillary zone electrophoresis. *Electrophoresis*, **16** (11), 2034–2038.